

Photonic Microwave Characteristics and Modeling of an $\text{Al}_{0.3}\text{Ga}_{0.7}\text{As}/\text{GaAs}/\text{In}_{0.13}\text{Ga}_{0.87}\text{As}$ Double Heterostructure Pseudomorphic HEMT

S. H. Song, *Student Member, IEEE*, D. M. Kim, *Member, IEEE*, H. J. Kim, S. H. Kim, K. N. Kang, *Member, IEEE*, and M. I. Nathan

Abstract—Electrical characteristics of a photonically controlled n-channel $\text{Al}_{0.3}\text{Ga}_{0.7}\text{As}/\text{GaAs}/\text{In}_{0.13}\text{Ga}_{0.87}\text{As}$ double heterostructure pseudomorphic HEMT (PHEMT) is reported. Experimental results show a high optical sensitivity in the drain saturation current, the transconductance f_T , and f_{max} at the optical power density $P_{\text{opt}} = 78 \text{ mW/cm}^2$. We also proposed a new optoelectronic equivalent circuit model, which has photonically generated gate capacitances ($C_{\text{gs,opt}}$ and $C_{\text{gd,opt}}$) and transconductance ($g_{m,\text{opt}}$), for accurate description of dc and microwave performance of PHEMT's under optical control, and verified the accuracy of the proposed model with measured and extracted scattering parameters from the equivalent photonic microwave model.

Index Terms—Equivalent circuit, HEMT, modeling.

I. INTRODUCTION

THE photonic control of microwave semiconductor devices has been a fast-growing research area since they have possible applications to the optoelectronic integrated circuits for high-speed photonic microwave signal processing in the optical communication systems [1]–[3]. A HEMT controlled by an external optical source includes the possibility of integrating field-effect transistors (FET's) and photonic devices on a single chip as a monolithic microwave integrated circuit to perform multiple circuit functions for high-performance optical communication systems. There have been enormous efforts to implement highly responsive photonic microwave systems on a single wafer with high-performance HEMT's [3], [4]. It is also necessary to characterize and model optically controlled microwave devices for efficient simulation and accurate prediction of performances in photonic microwave integrated systems.

In this letter, we report dc and microwave characteristics of the n-channel $\text{Al}_{0.3}\text{Ga}_{0.7}\text{As}/\text{GaAs}/\text{In}_{0.13}\text{Ga}_{0.87}\text{As}$ PHEMT under optical illumination. We also proposed and verified a new photonic microwave equivalent circuit model for better description of the HEMT's under optical control.

Manuscript received August 28, 1997.

S. H. Song and D. M. Kim are with the School of Electrical Engineering, Kookmin University, Seoul 136-702, Korea (e-mail: dmkim@kmu.kookmin.ac.kr).

H. J. Kim, S. H. Kim, and K. N. Kang are with the Photonics Research Center, KIST, Seoul 130-650, Korea.

M. I. Nathan is with the Department of Electrical Engineering, University of Minnesota, Minneapolis, MN 55455 USA.

Publisher Item Identifier S 1051-8207(98)00852-6.

TABLE I
THE EPITAXIAL STRUCTURE OF THE DOUBLE HETEROSTRUCTURE n-CHANNEL $\text{Al}_{0.3}\text{Ga}_{0.7}\text{As}/\text{GaAs}/\text{In}_{0.13}\text{Ga}_{0.87}\text{As}$ PSEUDOMORPHIC HEMT

Material	Doping [cm^{-3}]	Thickness [\AA]
GaAs	n ⁺ -type 5×10^{18} (Si)	300
$\text{Al}_{0.3}\text{Ga}_{0.7}\text{As}$	Undoped	500
$\text{Al}_{0.3}\text{Ga}_{0.7}\text{As}$	N-type 1×10^{18} (Si)	100
$\text{Al}_{0.3}\text{Ga}_{0.7}\text{As}$	Undoped	50
GaAs	Undoped	50
$\text{In}_{0.13}\text{Ga}_{0.87}\text{As}$	Undoped	100
GaAs	Undoped	50
$\text{Al}_{0.3}\text{Ga}_{0.7}\text{As}$	Undoped	50
$\text{Al}_{0.3}\text{Ga}_{0.7}\text{As}$	N-type 1×10^{18} (Si)	100
GaAs	Undoped	2000
Semi-Insulating (100) GaAs Substrate		

II. FABRICATION AND PHOTONIC CONTROL OF THE PSEUDOMORPHIC HEMT's

The epitaxial structure of the pseudomorphic HEMT was grown by a GSMBE and layers are shown in the Table I. Double heterojunction quantum-well structures were employed to obtain better carrier confinement and improved carrier transport in the pseudomorphic $\text{In}_{0.13}\text{Ga}_{0.87}\text{As}$ layer. We obtained $\mu_n = 5000 \text{ cm}^2/\text{V}\cdot\text{s}$ and $n_s = 1.2 \times 10^{12} \text{ cm}^{-2}$ for the 2-DEG's, which are characterized by the Hall measurement at 300 K. Physical dimension of the PHEMT has $L_g = 1 \text{ }\mu\text{m}$, $L_{\text{gs}} = L_{\text{gd}} = 1 \text{ }\mu\text{m}$, and $W = 200 \text{ }\mu\text{m}$ with V-shaped double-gate PHEMT structure, expecting better controllability and sensitivity for optoelectronic applications.

The optoelectronic performances of the fabricated PHEMT were characterized on wafer by combining the HP-4156A, the HP-8510B, and the Spectra-Physics laser diode module with $\lambda = 0.83 \text{ }\mu\text{m}$ for optical modulation of the PHEMT under study. As typical dc parameters of the PHEMT's characterized under saturation mode of gate and drain biases, we obtained the maximum drain saturation current $I_{\text{DSS}} = 12.0 \text{ mA}$ and the pinchoff voltage $V_P = -0.9 \text{ V}$. The maximum extrinsic transconductance and the drain output resistance were measured to be $g_{m(\text{max})} = 130 \text{ mS/mm}$ and $r_{\text{ds}} = 760 \text{ }\Omega$ without optical illumination. Under $P_{\text{opt}} = 78 \text{ mW/cm}^2$ of optical illumination on the device on-wafer state, which

is carried via multimode optical fiber from the laser diode module, we obtained $I_{DSS} = 23.5$ mA, $g_{m(\max)} = 155$ mS/mm, $r_{ds} = 40$ k Ω , and $V_P = -1.2$ V.

The effective pinchoff voltage change under optical illumination is expected to be caused by the photovoltaic effect which requires more negative gate voltage to turn-off the transistor due to photogenerated excess carriers [3]. The drain current at $V_{GS} = -0.7$ V in the saturation region of operation shows 2.9 mA compared with $I_{D(\text{sat})} = 0.2$ mA under no optical illumination. A significant increase in the drain current with the photonic input is mainly resulted from optically generated carriers in the GaAs spacer and pseudomorphic $\text{In}_{0.13}\text{Ga}_{0.87}\text{As}$ channel layer, which is expected to be the most responsive layer and contribute to the generation of excess electron-hole pairs for channel carriers under optical illumination of $\lambda = 0.83$ μm .

Even with a large increase in the drain saturation current under a photonic control, however, the maximum transconductance $g_{m(\max)}$ does not change so much with optical illumination. This is supposed to be mainly due to the increased effective channel length, $L_{g(\text{eff})}$ with optical illumination (which is larger than the metallurgical gate length), L_g and the effective channel length under no illumination. This is also verified by the dramatically increased output resistance— r_{ds} under illumination. In the two optically responsive regions of the PHEMT under optical illumination, one between the gate and the source and the other between the gate and the drain, optical illumination induces a high density of photoconductive excess carriers and makes them more conductive in the space regions; otherwise, they are counted as parasitic source and drain resistances. This is also verified by the reduced parasitic source and drain resistances (R_S, R_D) caused by both the enhanced photoconductivity and the reduced effective spacings with optical illumination.

III. PHOTONIC CONTROL OF MICROWAVE CHARACTERISTICS IN THE PHEMT

Microwave scattering parameters were measured on wafer by the HP8510B vector network analyzer up to 40 GHz after calibration process performed by the SOLT technique. During the photonic microwave characterization, the HP4156A was used for simultaneous biasing and measurement of current-voltage characteristics of the PHEMT under test.

The common-source current gain cutoff frequency (f_T) and the maximum frequency of oscillation (f_{\max}) were obtained from the current gain ($|h_{21}|$) and the unilateral power gain ($|U|$), respectively. Extrapolating $|h_{21}|$ and the $|U|$ curves to 0 dB, maximum values of the f_T and the f_{\max} were found to be 6.62 GHz at $V_{GS} = 0$ V and 3.32 GHz $V_{GS} = -0.7$ V, respectively, in the near pinched-off state of the PHEMT with $V_{DS} = 2.4$ V.

With an optical input power $P_{\text{opt}} = 78$ mW/cm², maximum values of the f_T and the f_{\max} were improved and measured to be 10.42 GHz at $V_{GS} = 0$ V and 4.44 GHz at $V_{GS} = -0.7$ V for the same $V_{DS} = 2.4$ V. The maximum value of the f_T was increased by 50% while the maximum of the f_{\max} was improved by 34% under the optical input. Bias-dependent

TABLE II
THE BIAS-DEPENDENT CURRENT GAIN CUTOFF FREQUENCY (f_T)
AND THE MAXIMUM FREQUENCY OF OSCILLATION (f_{\max})
UNDER OPTICAL ILLUMINATION $P_{\text{opt}} = 78$ mW/cm²

V_{DS} [V]	V_{GS} [V]	I_D [mA]		f_T [GHz]		f_{\max} [GHz]	
		Non-ill.	Ill.	Non-ill.	Ill.	Non-ill.	Ill.
0.5	0.0	9.2	17.2	4.07	5.30	0.382	-
	-0.3	5.12	13.3	3.98	6.95	1.65	-
	-0.7	0.14	2.73	0.843	5.30	2.8	3.40
2.4	0.0	14.0	21.8	6.62	10.4	2.52	4.07
	-0.3	7.73	15.78	5.24	9.35	2.75	4.12
	-0.7	0.14	2.73	1.51	5.73	3.32	4.44

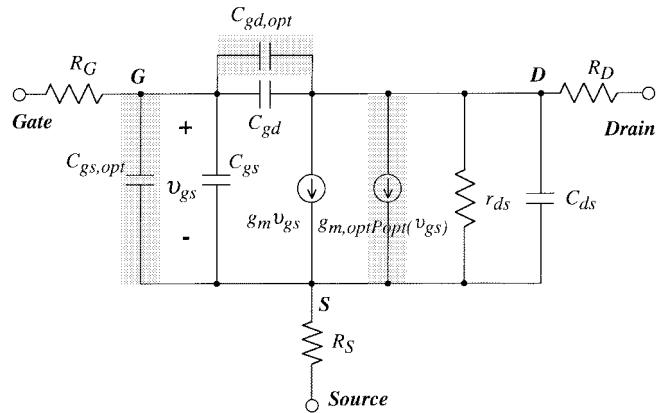


Fig. 1. A new photonic microwave equivalent circuit model with the optical diffusion capacitances ($C_{gs, \text{opt}}, C_{gd, \text{opt}}$) and the photonic transconductance ($g_{m, \text{opt}}$) in the optically controlled PHEMT.

performances of the characterized PHEMT are summarized in the Table II as a function of V_{GS} and V_{DS} . Experimental results in the Table II show that the f_T strongly depends on V_{DS} and V_{GS} both in the linear region and saturation region, even though f_T is almost constant over the saturation region for a given V_{GS} . The maximum frequency of oscillation f_{\max} also strongly depends on the V_{DS} both in the linear and saturation regions.

Contrary to the variation of the f_T with V_{GS} , the f_{\max} doesn't change so much with the gate-to-source bias V_{GS} , especially under the saturation mode operation. This can be explained by the photonic control effect on the channel carrier concentration, parasitic resistances, and capacitances in the n-channel PHEMT under optical illumination. Because the f_T is predominantly decided by the drain current via the transconductance g_m , the total gate capacitance $C_g = C_{gs} + C_{gd}$, and the intrinsic transit time of carriers limited by the gate length, the dominant contribution to the improvement in the f_T comes from the improved transconductance with optically generated excess carriers in the pseudomorphic InGaAs channel. Considering almost constant f_T with V_{DS} observed in the saturation mode of operation, dominant parameters limiting the f_T of the PHEMT under optical illumination are supposed to be the transconductance and the drain current for a given operating point.

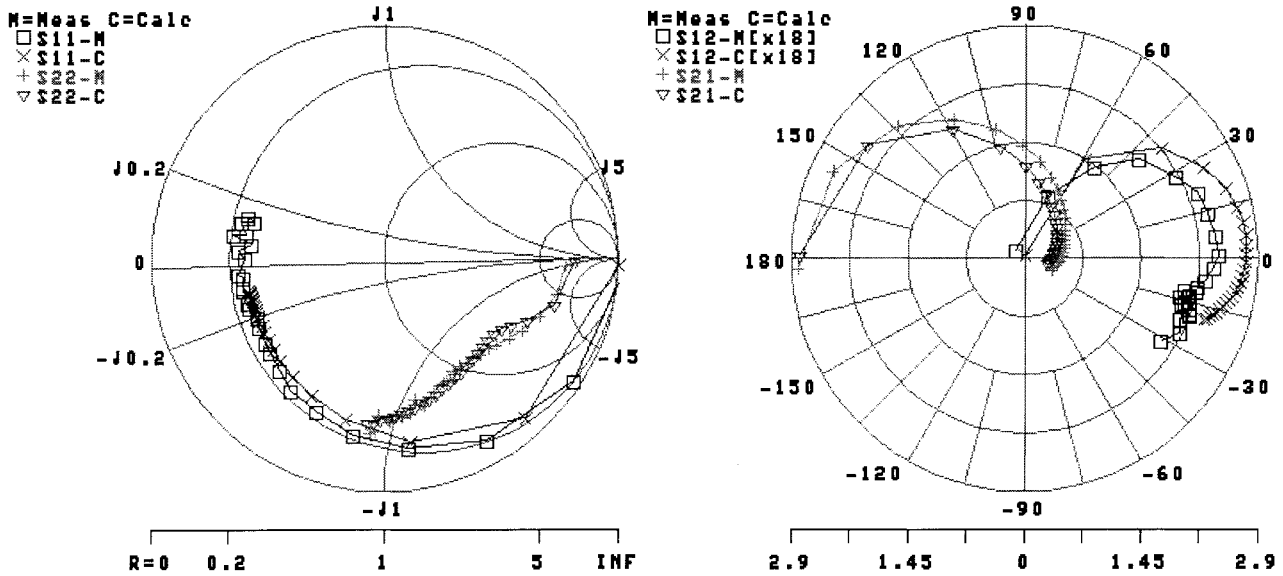


Fig. 2. Measured and simulated microwave characteristics of the PHEMT ($F = 45 \text{ MHz}$ to 40 GHz) biased at $V_{GS} = -0.3 \text{ V}$ and $V_{DS} = 1.0 \text{ V}$. The simulated result obtained from the proposed equivalent circuit model with the optical diffusion capacitances ($C_{gs, opt}$, $C_{gd, opt}$) and the photonic transconductance ($g_{m, opt}$).

We also note that the most dominant limiting element in the f_{max} under optical input is parasitic gate capacitance. Considering these experimental observations, we proposed a new optoelectronic equivalent circuit model for photonic microwave characteristics of the PHEMT as shown in Fig. 1. We included new model parameters, called the optical diffusion capacitance (C_{opt}) and the photonic transconductance ($g_{m, opt}$). The C_{opt} , parallel to the gate-to-source depletion capacitance (C_{gs}) which decreases with $-V_{GS}$ but independent of the P_{opt} , increases with the P_{opt} due to increased excess carriers under optical illumination, but independent of the electrical gate-to-source bias V_{GS} . We also included photonic transconductance ($g_{m, opt}$), which solely depends on the optical input, parallel to the electrical transconductance (g_m), which is determined by the electrical biases V_{GS} and V_{DS} .

We verified the accuracy of the new model containing the optical diffusion capacitance and the photonic transconductance. Without optical input, we obtained $R_D = 5.9 \Omega$, $R_S = 2.5 \Omega$, $R_G = 11.7 \Omega$, $C_{gs} = 0.54 \text{ pF}$, $C_{gd} = 0.29 \text{ pF}$ in the equivalent circuit. With these model parameters, microwave scattering parameters were matched well with measured microwave characteristics. Under optical input of $P_{opt} = 78 \text{ mW/cm}^2$ for the PHEMT with a gate capacitance $C_{gs} = 0.54 \text{ pF}$, we obtained $g_{m, opt} = 25 \text{ mS/mm}$, $C_{gs, opt} = 0.15 \text{ pF}$, and $C_{gd, opt} = 0.07 \text{ pF}$. We also obtained $R_D = 3.3 \Omega$, $R_S = 2.3 \Omega$, $R_G = 9.9 \Omega$, $C_{gs} = 0.54 \text{ pF}$, and $C_{gd} = 0.29 \text{ pF}$ as model parameters under optical illumination. Parasitic resistances are reduced while the total gate capacitance is increased under optical input. Changes in the parasitic elements in the photonic microwave equivalent circuit are due to photovoltaic and photoconductive effects under optical input. Simulated microwave characteristics with new photonic microwave model for the optically controlled PHEMT agree well with experimental scattering parameters as shown in Fig. 2.

IV. CONCLUSION

In this work, we investigated photonic microwave characteristics of an n-channel $\text{Al}_{0.3}\text{Ga}_{0.7}\text{As}/\text{GaAs}/\text{In}_{0.13}\text{Ga}_{0.87}\text{As}$ PHEMT. DC and microwave characteristics of the PHEMT with V-shaped double gate structure are characterized with laser diode module: $\lambda = 0.83 \mu\text{m}$. For the optoelectronic microwave characterization, $P_{opt} = 78 \text{ mW/cm}^2$ was applied to the PHEMT on wafer. With the optical illumination, the PHEMT shows a significant change in the dc and microwave performance parameters such as the maximum drain saturation current (I_{DSS}), the transconductance (g_m), the current gain cutoff frequency (f_T), and the maximum frequency of oscillation (f_{max}). Physical mechanisms contributing to the variation of those performance parameters mainly came from the increased photoconductivity and the photovoltaic effect of the channel and reduced parasitic resistances due to optically generated excess carriers. In addition, we verified that the optical diffusion capacitances ($C_{gs, opt}$ and $C_{gd, opt}$) and photonic transconductance ($g_{m, opt}$) should be included in the conventional equivalent circuit model for better description of the photonic microwave characteristics of the PHEMT under optical illumination.

REFERENCES

- [1] W. R. Robertson, *Optoelectronic Techniques for Microwave and Millimeter-Wave Engineering*. Boston, MA: Artech House, 1995.
- [2] R. N. Simon, "Microwave performance of an optically controlled AlGaAs/GaAs high electron mobility transistor and GaAs MESFET," *IEEE Trans. Microwave Theory Tech.*, vol. MTT-35, p. 1444, Dec. 1987.
- [3] M. A. Romero, M. A. G. Martinez, and P. R. Herczfeld, "An analytical model for the photodetection mechanisms in high-electron mobility transistors," *IEEE Trans. Microwave Theory Tech.*, vol. 44, pp. 2279-2287, Dec. 1996.
- [4] B. B. Pal and S. N. Chattopadhyay, "GaAs OPFET characteristics considering the effect of gate depletion with modulation due to incident radiation," *IEEE Trans. Electron Devices*, vol. 39, p. 1021, May 1992.